HHS Public Access

Author manuscript

Circ Cardiovasc Imaging. Author manuscript; available in PMC 2016 April 01.

Published in final edited form as:

Circ Cardiovasc Imaging. 2015 April ; 8(4): . doi:10.1161/CIRCIMAGING.114.002979.

AUGMENTATION OF LIMB PERFUSION AND REVERSAL OF TISSUE ISCHEMIA PRODUCED BY ULTRASOUND-MEDIATED MICROBUBBLE CAVITATION

J. Todd Belcik, RCS, RDCS[*], **Brian H. Mott, MD**[*], **Aris Xie, MS**[*], **Yan Zhao, MD**[*], **Sajeevani Kim, MD**[*], **Nathan J. Lindner**[*], **Azzdine Ammi, PhD**[*], **Joel M. Linden, PhD**[†], and **Jonathan R. Lindner, MD**[*]

[*]Knight Cardiovascular Center, Oregon Health & Science University, Portland, OR

[†]La Jolla Immunology and Allergy Institute, La Jolla, CA

Abstract

Background—Ultrasound can increase tissue blood flow in part through the intravascular shear produced by oscillatory pressure fluctuations. We hypothesized that ultrasound-mediated increases in perfusion can be augmented by microbubble contrast agents that undergo ultrasound-mediated cavitation, and sought to characterize the biologic mediators.

Methods and Results—Contrast ultrasound perfusion imaging of hindlimb skeletal muscle and femoral artery diameter measurement were performed in non-ischemic mice after unilateral 10 min exposure to intermittent ultrasound alone (mechanical index [MI] 0.6 or 1.3) or ultrasound with lipid microbubbles (2×10^8 I.V.). Studies were also performed after inhibiting shear- or pressure-dependent vasodilator pathways, and in mice with hindlimb ischemia. Ultrasound alone produced a 2-fold increase ($p<0.05$) in muscle perfusion regardless of ultrasound power. Ultrasound-mediated augmentation in flow was greater with microbubbles (3-fold and 10-fold higher than control for MI 0.6 and 1.3, respectively; $p<0.05$), as was femoral artery dilation. Inhibition of endothelial nitric oxide synthase (eNOS) attenuated flow augmentation produced by ultrasound and microbubbles by 70% ($p<0.01$), whereas inhibition of adenosine-A_{2a} receptors and epoxyeicosatrienoic acids had minimal effect. Limb nitric oxide (NO) production and muscle phospho-eNOS increased in a stepwise fashion by ultrasound and ultrasound with microbubbles. In mice with unilateral hindlimb ischemia (40–50% reduction in flow), ultrasound (MI 1.3) with microbubbles increased perfusion by 2-fold to a degree that was greater than the control non-ischemic limb.

Conclusions—Increases in muscle blood flow during high-power ultrasound are markedly amplified by the intravascular presence of microbubbles and can reverse tissue ischemia. These effects are most likely mediated by cavitation-related increases in shear and activation of eNOS.

Correspondence to: Jonathan R. Lindner, MD, Cardiovascular Division, UHN 62, Oregon Health & Science University, 3181 SW Sam Jackson Park Road, Portland, OR 97239, P – (503) 494-8750, F – (503) 494-8550, lindnerj@ohsu.edu.

Disclosures

None.

Keywords

contrast ultrasound; microbubbles; muscle perfusion; nitric oxid; peripheral artery disease

Ultrasound has been used for a wide variety of therapeutic applications. The ability to acutely augment tissue perfusion with ultrasound has led to interest in its use to treat tissue ischemia in cardiovascular disease. Low-frequency (<100 MHz) ultrasound has been shown to produce peripheral and coronary artery dilation in animal models and in humans,[1–4] and to increase tissue perfusion in animal models of limb or myocardial ischemia.[5–7] Both thermal and non-thermal bioeffects are thought to contribute to ultrasound-mediated vasodilation. The most important non-thermal effect is the convective motion, or microstreaming, that can produce shear-mediated endothelial production of nitric oxide (NO).[8] Over a wide range of frequencies (27 kHz to 1.0 MHz) ultrasound has been shown to promote *in vitro* endothelial cell NO production in a power-dependent fashion.[9–11] In the *in vivo* setting, ultrasound-mediated vasodilation and augmentation in tissue blood flow are reduced, although not completely blocked, by inhibitors of endothelial nitric oxide synthase (eNOS).[4–6]

The presence of gas bodies such as encapsulated microbubble (MB) contrast agents within the vasculature can amplify shear-mediated bioeffects. Concentrated wall shear stresses result from stable and inertial cavitation produced by non-linear oscillation of MBs in an acoustic field.[8,12] High-power ultrasound with MBs has been shown to augment capillary perfusion on intravital microscopy and to reduce ischemic damage in a porcine model of acute myocardial infarction presumably through effects on myocardial blood flow.[13–15] In this study we sought to quantify the degree to which ultrasound's effects on vascular tone and tissue perfusion in normal and ischemic tissues are influenced by the presence of MBs. We also sought to characterize the biologic mediators responsible for increased perfusion during MB insonification by examining an array of compounds that can mediate vasodilation in response to vascular shear and/or pressure such as adenosine and the epoxyeicosatrienoic acid (EET) family of endothelial hyperpolarizing factors formed from cytochrome P450 metabolism of arachadonic acid.[16,17]

Methods

Animal Preparation

The study protocol was approved by the Institutional Animal Care and Use Committee at Oregon Health & Science University. Male C57Bl/6 mice 8 to 12 weeks of age were studied. Mice were anesthetized with 1.0–1.5% inhaled isoflurane. Body temperature was maintained at 37° C with a heating platform. A jugular vein was cannulated for administration of microbubbles. Studies were performed in a subset of mice (n=12) with chronic hindlimb ischemia. Ischemia was produced by unilateral ligation of the distal common iliac artery and the origin of the epigastric artery through a midline abdominal incision and imaging studies were performed at 21–25 days after surgery at a time where flow recovery from endogenous vascular remodeling has completed resulting in a 40–50% reduction of resting flow.[18]

Therapeutic Ultrasound Exposure Protocols

For non-ischemic mice, the proximal adductor muscles of the left hindlimb were exposed to therapeutic ultrasound for 10 min. The transducers were placed at a fixed distance (3 cm) from the mid-portion of the muscle using a transverse imaging plane. Ultrasound was performed over 10 min using harmonic power-Doppler imaging (Sonos 7500, Philips Ultrasound, Andover, MA) at 1.3 MHz, a pulse repetition frequency of 9.3 kHz, and a mechanical index (MI) of either 0.6 or 1.3. For experiments performed with MBs, lipid-shelled decafluorobutane MBs with a mean diameter of 2.0–2.5 μm were prepared.[19] Microbubbles (2×10^8) were suspended in 100 μL of volume and administered over the first minute of ultrasound exposure. The following experimental conditions were tested: (**a**) intermittent ultrasound (pulsing interval of 5 s) without MBs at an MI of 0.6 (n=4) or 1.3 (n=7 each); (**b**) intermittent ultrasound with MBs at an MI of 0.6 or 1.3 (n=4 each); and (**c**) continuous (frame rate 16 Hz) ultrasound at an MI of 1.3 (n=5). High MI experiments with MBs were also performed after inhibiting vasodilator pathways with the following conditions (n=5 for each): (**a**) inhibiting eNOS with L-nitroarginine methyl ester (L-NAME, Santa Cruz Biotech., Santa Cruz, CA; 75 μg/kg I.P. 30 min prior to study); (**b**) inhibiting adenosine A_{2a}-receptors with 4-(2-[7-Amino-2-(2-furyl)[1,2,4]triazolo[2,3-a] [1,3,5]triazin-5-ylamino]ethyl)phenol (ZM-241385, Abcam PLC, Cambridge, MA; 50 μg/g I.V., 1 hr prior to study); and (**c**) inhibiting EETs with 14,15-epoxyeicosa-5(Z)-enoic acid (EEZE, Cayman Chemical Co., Ann Arbor, MI; 2.5 μg/g I.V., 1 hr prior to study). The effect of using a lower microbubble concentration was also assessed by performing intermittent high-MI (1.3) imaging after intravenous injection of 1×10^6 microbubbles (n=4). The acoustic pressure at the focus (corresponding to the mid portion of the muscle) was spatially quantified by a 0.075 mm needle hydrophone (Precision Acoustics) with 500 μm steps in the lateral and elevational direction. For mice with unlitateral ischemia, only the ischemic limb was exposed to intermittent ultrasound at an MI of 1.3.

Microvascular Perfusion Imaging

Contrast-enhanced ultrasound perfusion imaging of the proximal hindlimb adductor muscles of the therapeutic ultrasound-exposed and contralateral control limb was performed.[20] For non-ischemic animals, perfusion imaging was performed only after therapeutic ultrasound exposure and data acquisition was performed between 10 and 15 min after completion of therapy. For mice with unilateral hindlimb ischemia, perfusion in both limbs was assessed at baseline 21–23 days after arterial ligation, and again after therapeutic ultrasound which was performed 3 days later so as to minimize the potential effects of baseline perfusion imaging. The non-linear fundamental signal component from MBs was detected using multipulse phase-inversion and amplitude-modulation (Sequoia 512, Siemens Medical Systems, Mountain View, CA) at 7 MHz and an MI of 0.18. Microbubbles were infused at a rate of 1×10^7 min^{-1}. Time-intensity data at a frame rate of 5 Hz were acquired after a high-power (MI 0.98) 5-frame sequence and were fit to the function: $y=A(1-e^{\beta t})$; where y is intensity at time t, A is the plateau intensity representing relative microvascular blood volume, and the rate constant β is the microvascular flux rate.[21] Microvascular blood flow (MBF) was quantified by the product of A and β.[21]

Arterial Dilation

Bilateral femoral artery dimension was measured before and immediately after therapeutic US exposure in the same mice undergoing perfusion imaging. The femoral artery was imaged with a high-frequency ultrasound imaging system (Vevo-770, VisualSonics, Toronto, Ontario, Canada) at 55 MHz. Bilateral femoral artery diameter was measuring using an inner edge-to-edge technique at baseline and upon completion of therapeutic ultrasound exposure.

Muscle NO Production and Temperature

Phosphorylation of eNOS was evaluated in muscle samples obtained from within the ultrasound beam (MI 1.3) with and without MBs, and non-exposed muscle (n=5 each). Samples were obtained immediately upon completion of post-exposure perfusion imaging. Samples were homogenized in lysis buffer containing 1mM phenylmethylsulfonyl fluoride, centrifuged, and the supernatant was evaluated for phosphorylated eNOS using an enzyme-linked immunosorbent assay (PathScan ELISA, Cell Signaling Tech.).

Continuous *in situ* measurements of skeletal muscle NO concentration and temperature were also performed but in a separate group of mice due to the attenuating effect of the catheters on perfusion imaging. Catheters (600 μm tip) housing a thermistor and an amperometric electrochemical sensing element (amino-IV, Innovative Instruments, Tampa, FL) were interfaced with an A/D converter (inNO-T-II, Innovative Instruments) and calibrated for NO concentration.[22] The catheters were inserted into the hindlimb adductor muscles bilaterally. Once measurements reached steady state (approximately 10 min), measurements were acquired at baseline and then continuously after starting unilateral intermittent high-power (MI 1.3) ultrasound with or without MB (n=6 for each condition). In four of the animals receiving MBs, measurements were continued for 10 min after cessation of ultrasound. Intramuscular temperature over the course of the procedure was measured from the same catheters. In two additional mice, high-power ultrasound with MB was performed after pre-treatment with L-NAME (75 mg/Kg I.P. 30 min before ultrasound exposure) to verify that signal changes were attributable to changes in NO concentration.

Endothelial Cell NO Production

Murine endothelial cells (SVEC4-10, ATCC, Manassas, VA) were grown to confluence in DMEM supplemented with 10% fetal bovine serum on fibronectin-coated culture dishes. The fluorescent indicator 4,5-diaminofluorescein diacetate (DAF-2, Cayman Chemical Co.) was added to the medium and culture dishes were placed in an inverted position to allow MB flotation to the cell surface. Fluorescence intensity was measured by microscopy with a silicone-intensified tube camera (SIT68, Dage-MTI, Michigan City, IN) during brief fluorescent illumination (460–500 nm excitation). Intensity was measured in 8 separate optical fields within the ultrasound sector at baseline and 10 min after the following conditions: (**a**) no ultrasound; (**b**) ultrasound (PI 5 s, MI 1.3, 45-degree incident angle); (**c**) ultrasound and MB (1×10^5 mL^{-1}).

Histology

In animals not undergoing hindlimb ischemia, mice were recovered after perfusion imaging and muscle samples from all ultrasound and MB conditions were obtained from within and outside the ultrasound beam at either 90 min after completion of therapeutic ultrasound for evaluating acute effects, or at three days after exposure for evaluating inflammatory response (n=3 for each). Immersion fixed and paraffin embedded sections were stained with hematoxylin and eosin for evidence of vascular rupture, myocyte edema, and inflammatory cell infiltration.

Microbubble Cavitation

Characterization of microbubble cavitation during ultrasound exposure (1.8 MHz) at a MI of 0.6 and 1.3 was assessed by passive cavitation detection (PCD). A spherically focused broadband (10 KHz to 20 MHz) hydrophone (Y-107, Sonic Concepts, Inc., WA) with a focal depth of 20 mm and a focal width of 0.4 mm was confocally positioned with the therapeutic ultrasound transducer at a 70° relative angle to receive signals from a flow phantom containing microbubbles (1×10^6 mL^{-1}). Received signals were digitized (25 MHz) and saved in a 4-channel oscilloscope (Waverunner, Teledyne LeCroy, Chestnut Ridge, NY) using sequence mode. Data analysis for 250 exposures for each condition was performed with the Matlab (MathWorks, Natick, MA).

Statistical Analysis

Data are expressed as ±SD unless stated otherwise. D'Agostino and Pearson omnibus test were used to assess data normality. Significance for variance among groups was analyzed with one-way ANOVA and when significant ($p<0.05$), post-hoc analysis was performed with paired (pre- vs. post-exposure; treated vs. untreated leg) or unpaired (comparisons between treatment groups) Student's *t*-test with Bonferroni's correction. Non-normally distributed data were analyzed with a Mann-Whitney or Wilcoxon signed rank test. Correlations were made by linear regression analysis. Comparisons between relationships for NO biosensor data were made by non-paired Student's t-test of the individual slopes.

Results

Ultrasound-mediated Augmentation in Perfusion

The therapeutic ultrasound beam peak rarefactional acoustic pressures for the lateral and elevational dimensions are provided in Figure 1. These data indicate that approximately 40% and 80% of the adductor muscle group was exposed to ultrasound when imaging in a transverse plane at an MI of 0.6 and 1.3, respectively.

For non-ischemic mice, the mean microvascular blood flux rate (β) and microvascular blood flow (MBF) of the adductor muscle group in the control contralateral limb not exposed to ultrasound was not significantly different between treatment groups (Figure 2). Ten minutes of intermittent or continuous ultrasound exposure without MBs produced a significant increase in both β and MBF compared to the contralateral non-exposed limb, although the degree of change did not meet statistical significance when ultrasound was delivery continuously. During intermittent ultrasound exposure, both β and MBF were greater in the

presence of MBs, particularly at the higher acoustic pressure (MI 1.3). Qualitatively, the increase in perfusion in the muscle was diffusely distributed. There was no evidence for any petechial hemorrhage at the ultrasound exposure site on gross inspection or by histology, nor was there an inflammatory cell infiltration either acutely or at three days (Supplemental Figure 1). Intermittent high-power (MI 1.3) exposure of a much lower dose of microbubbles (1×10^6) resulted in a substantial reduction in the degree of flow augmentation indicating that changes in perfusion are not only pressure-related but also microbubble dose-related. (Supplemental Figure 2)

Measurement of femoral artery diameter bilaterally by high-frequency ultrasound could be made pre- and post-exposure in all but one of the non-ischemic mice (assigned to ultrasound at MI 0.6 with MB). Ultrasound produced femoral artery dilation in all groups, the degree of which tended to be greater in the presence of MBs (Figure 3).

Perfusion Augmentation in Ischemic Limbs

In mice with chronic ischemia, baseline adductor muscle perfusion was assessed a mean of 23±3 days after after ligation (Figure 4). Muscle blood flow was reduced by 40–50% compared to that in the contralateral control limb, attributable largely to a reduction in β. Three days later, MBF and β measured after exposure to ultrasound (MI 1.3) with MBs was not only significantly greater than baseline and had increased to a level higher than the control limb.

Inhibition of the Vascular Effect of Ultrasound and Microbubbles

The contribution of different shear- or pressure-activated vasodilators to the augmentation of perfusion during high-power (MI 1.3) ultrasound with MBs was investigated by inhibition of key vasodilator pathways in non-ischemic mice (Figure 5). In the ultrasound-exposed limb, the increase in both both MBF and β produced by ultrasound and MBs was significantly blunted by inhibition of eNOS with L-NAME. Within the L-NAME treatment group, both β and MBF were still significantly ($p<0.05$) higher in the exposed compared to the contralateral control leg, suggesting incomplete inhibition of the vascular effects of ultrasound and MB. However, L-NAME did completely abolish femoral arterial dilation (0% increase from pre- to post-exposure in both limbs). Neither ZM-241385 nor EEZE significantly reduced post-exposure MBF. However, because both ZM-241385 and EEZE MBF produced a small increase in flow in the control non-exposed limb, the ratio of MBF in the exposed to non-exposed leg was lower than that in animals that did not receive any blocking intervention (11.5±4.1 in controls; 4.8±4.5 for ZM-241385 [p=0.07 vs. control]; 5.7±3.6 for EEZE [p=0.10 vs. control]).

Ultrasound-mediated Changes in NO and Temperature

To further characterize whether the presence of MBs enhances ultrasound-mediated release of NO, three separate experiments were performed. First NO production by cultured SVECs was assessed by DAF-2 chemifluorescence (Figure 6A). Ten minutes of high-power ultrasound (MI 1.3) exposure resulted in a greater increase in DAF-2 intensity compared to non-exposed time-controlled condition, the extent of which was greater in the presence of MBs. Phosphorylation of eNOS *in vivo* in ultrasound-exposed muscle also showed increased

phospho-eNOS in the presence of MBs (Figure 6B). Nitric oxide production quantified *in vivo* by an indwelling electrochemical sensor detected a continuous increase in NO concentration over a 10 min period of intermittent high-power ultrasound which was much greater for animals receiving MBs (Figure 7A). In animals pre-treated with L-NAME, there were no significant changes in NO concentration during high-power ultrasound exposure of MBs. In animals receiving MB, production of NO remained elevated without further increase for ten minutes after cessation of ultrasound ultrasound (Figure 7B). Temperature in the ultrasound-exposed limb increased only slightly in animals receiving MB but not in those without MB (+0.69±0.30 vs. −0.10±0.54° C, p=0.01).

Cavitation Detection

Microbubble cavitation was characterized by PCD using the two different acoustic conditions applied *in vivo*. The degree of inertial cavitation in these studies was defined as the broad-band signal seen between higher-order harmonic peaks (either absolute amplitude or relative to harmonic peaks). A modest amount of inertial cavitation was present at an MI of 0.6 (Figure 8). The degree of inertial cavitation increased substantially when the MI was increased to 1.3.

Discussion

There is growing interest in the use of non-invasive therapeutic ultrasound to augment perfusion in acute or chronic ischemia that occurs in cardiovascular disease. In this study we have for the first time quantified the degree to which MB contrast agents amplify this effect. We have demonstrated that presence of MBs within the microcirculation markedly enhance ultrasound-mediated augmentation in muscle MBF, particularly when ultrasound is administered at high acoustic power. We have also demonstrated that this approach can reverse moderate tissue ischemia in a model of chronic peripheral arterial disease. Flow augmentation with ultrasound and MBs appears to be mediated primarily by NO with only minor contributions from other vasodilator pathways.

Part of the beneficial therapeutic effects of ultrasound in tissue repair and healing are thought to be attributable to local effects on perfusion.[23] Accordingly, there has been interest in applying therapeutic ultrasound in ischemic cardiovascular disease. Low-frequency ultrasound has been shown to improve tissue perfusion in animal models of both limb and myocardial ischemia.[5,7] It has recently been reported that higher frequency (>1.0 MHz) ultrasound used in combination with MB contrast agents in porcine models of acute coronary thrombosis reduce myocardial injury and possibly infarct size, even when the intended effect of epicardial recanalization does not occur.[14,15] This finding could relate to arteriolar vasodilation seen on intravital microscopy of the hamster cheek pouch after ultrasound exposure of MBs.[13] These observations formed the foundation of our present efforts to determine the degree to which MB contrast agents augment ultrasound's effects on tissue perfusion *in vivo*.

Although performed in mice, our studies evaluated the effects of MBs at dose equivalents that are either well under or above the currently-approved dose for use in humans. We also chose to use ultrasound at frequencies and acoustic pressures that are well within the

approved ranges for diagnostic cardiovascular ultrasound even when scaled for human use. Because ultrasound-mediated cavitation of MBs at high MI results in their destruction within the vascular compartment,[24] ultrasound was delivered using a pulsing interval that would ensure nearly complete replenishment of MBs into skeletal muscle between sequential ultrasound exposures.[20] During high-power ultrasound the presence MBs increased tissue perfusion in normal muscle by approximately 10-fold which was several times greater than that achieved with ultrasound alone whether administered in a pulsed or continuous fashion. For conditions without microbubbles, we included both intermittent and continuous ultrasound since previous studies demonstrating increases in perfusion with ultrasound alone used high duty factors. Our data indicate that the degree of flow augmentation is dependent on both acoustic pressure amplitude and microbubble concentration. With regards to pressure dependency, our PCD data suggest that the greater flow augmentation at the higher MI (1.3) was likely attributable to the greater degree of inertial cavitation.

The high-power ultrasound and high microbubble concentration conditions also produced a significant increase in MBF in animals with chronic hindlimb ischemia, albeit to a lesser extent than in non-ischemic mice. Yet, the degree of flow augmentation in ischemic limbs was of sufficient magnitude that MBF exceeded that in the normal contralateral control limb. It is also important to note that since our perfusion imaging protocols generally required ten to fifteen minutes to perform, we are assured that augmentation in flow persists after cessation of therapeutic ultrasound. Past studies have not been entirely consistent with regards to the duration of the beneficial effects of ultrasound on perfusion and there are likely to be differences in limb skeletal muscle and myocardium. Based on our previous experience sequentially examining perfusion in ischemic hindlimbs,[25] we not believe that the baseline perfusion imaging protocol performed three days prior to therapeutic exposure produced any angiogenic response in the ischemic limbs.

Ultrasound has been shown to produce brachial artery dilation in humans.[2] It is not clear whether this occurs from primary effects of ultrasound on the artery or secondary to flow-mediated dilation from ultrasound's effects on the distal microcirculation which could reduce distal microvascular resistance. In our study, we found that the presence of MB did indeed further augment arterial dilation, but not nearly to the degree to which perfusion was augmented. These data could support the notion that MB cavitation is selectively producing effects at the microvascular level and that large vessel dilation is permissive so as not to provide resistance to downstream flow regulation.[26,27] However, this supposition may not necessarily be true since vessel resistance is predicted to be related to the fourth power of its radius so that small differences in the degree of arterial vasodilation may have been amplified in terms of their effects on distal tissue perfusion.

Our studies were designed to test the mechanisms by which ultrasound cavitation of MBs produce changes in flow. Ultrasound exposure of muscle *in vivo* has been shown to result in phosphorylation of eNOS and generation of NO.[3,6,10] Inhibition of NOS has been shown to blunt ultrasound's effect of increasing myocardial perfusion during coronary occlusion.[5] Our results with L-NAME suggest that NO is a major but not the only pathway by which MB cavitation increases limb perfusion. We also demonstrated that both NO production and

eNOS phosphorylation increased incrementally with the addition of MBs to high power ultrasound. These data support the notion that MB cavitation acts to potentiate shear-mediated endothelial response. Intramuscular NO biosensors demonstrated that the production of NO occurred almost immediately after initiation of US and was sustained even after the period of therapeutic US. Unfortunately, the NO sensing probes are suited to measuring acute changes in NO concentration and do not provide sufficient stability or quantitation to have been able to measure NO for longer periods of time. They also could have potentially detected reactive oxygen species including oxidatively-modified NO in the form of peroxynitrate. In aggregate, our data support the notion that MB cavitation acts to potentiate shear-mediated endothelial response. The frequency-amplitude response on PCD further supports this notion since increased inertial cavitation produced by the higher MI (1.3) would be expected to produce higher shear, thereby explaining the greater augmentation in flow at the higher acoustic pressure. Although our temperature data suggest that MB cavitation produces a thermal effect, the very mild degree of heating would not be expected to produce MBF changes to the degree seen.[28]

Although femoral artery dilation during ultrasound with MBs was abolished by L-NAME, the increase in microvascular perfusion was not entirely abolished. This finding suggests that there may be mechanisms other than NO that also contribute to cavitation-related flow augmentation. Through inhibitory studies, we tested the contribution of adenosine and EETs which are formed in response to shear.[16] Although post-exposure flow was not reduced by inhibiting these pathways, baseline flow was higher in these studies so that flow reserve was signficiantly reduced, particularly with adenosine. It is unclear why baseline blood flow was higher after giving the A2a-receptor antagonist ZM241385 since this agent has not been shown to affect resting muscle blood flow in the cat.[29]

There are several limitations of the study that should be mentioned. Although the flow response to MB cavitation increases with ultrasound MI, we cannot state with absolute certainty that this effect was from higher pressure rather than a larger territory of muscle coverage. We also must be mindful that contrast ultrasound perfusion imaging was used as an endpoint and could have affected flow. For this reason, perfusion imaging in non-ischemic mice was performed only after therapeutic ultrasound and comparisons were made between the exposed and contralateral non-exposed limb. We believe that any effects in the contralateral limb were probably negligible given the minimal change in femoral artery diameter, and because in mice undergoing hindlimb ischemia, no major differences in flow were seen in the contralateral control leg for pre- and post-exposure conditions. It should be mentioned that brief high-frequency vascular imaging was used prior to therapeutic US exposure. However, these conditions were the same in both the control and therapeutic US-exposed limb and we have previously demonstrated that this type of exposure does not substantially alter muscle perfusion. Although we have used two drastically different microbubble doses, finer dose ranging studies will be necessary in the future. Finally, in the ischemic limbs we chose to only study the conditions that were found to produce the greatest results in non-ischemic animals.

In summary, for the first time we have quantified that extent to which MB cavitation augments ultrasound-mediated hyperemia and demonstrated that this approach can acutely

reverse tissue ischemia in a model peripheral artery disease. This approach represents a potential approach for acutely increasing blood flow in patients with critical limb ischemia who do not have recourse to immediate revascularization. The clinical translation of this technology will need further characterization of the duration of effect and efficacy with different degrees of tissue ischemia.

Supplementary Material

Refer to Web version on PubMed Central for supplementary material.

Acknowledgments

Sources of Funding: Dr. Mott is supported by a Ruth L. Kirschstein National Research Service Award (T32-HL094294); Dr. Ammi is supported by grant R01-HL095868; and Dr. Lindner is supported by grants R01-HL-078610 and R01-HL-111969 from the National Institutes of Health, Bethesda, Maryland; and a grant from the Doris Duke Charitable Foundation.

References

1. Steffen W, Cumberland D, Gaines P, Luo H, Nita H, Maurer G, Fishbein MC, Siegel RJ. Catheter-delivered high intensity, low frequency ultrasound induces vasodilation in vivo. Eur Heart J. 1994; 15:369–376. [PubMed: 8013511]
2. Iida K, Luo H, Hagisawa K, Akima T, Shah PK, Naqvi TZ, Siegel RJ. Noninvasive low-frequency ultrasound energy causes vasodilation in humans. J Am Coll Cardiol. 2006; 48:532–537. [PubMed: 16875980]
3. Atar S, Siegel RJ, Akel R, Ye Y, Lin Y, Modi SA, Sewani A, Tuero E, Birnbaum Y. Ultrasound at 27 khz increases tissue expression and activity of nitric oxide synthases in acute limb ischemia in rabbits. Ultrasound Med Biol. 2007; 33:1483–1488. [PubMed: 17507145]
4. Maruo A, Hamner CE, Rodrigues AJ, Higami T, Greenleaf JF, Schaff HV. Nitric oxide and prostacyclin in ultrasonic vasodilatation of the canine internal mammary artery. Ann Thorac Surg. 2004; 77:126–132. [PubMed: 14726048]
5. Siegel RJ, Suchkova VN, Miyamoto T, Luo H, Baggs RB, Neuman Y, Horzewski M, Suorsa V, Kobal S, Thompson T, Echt D, Francis CW. Ultrasound energy improves myocardial perfusion in the presence of coronary occlusion. J Am Coll Cardiol. 2004; 44:1454–1458. [PubMed: 15464327]
6. Suchkova VN, Baggs RB, Sahni SK, Francis CW. Ultrasound improves tissue perfusion in ischemic tissue through a nitric oxide dependent mechanism. Thromb Haemost. 2002; 88:865–870. [PubMed: 12428107]
7. Suchkova VN, Baggs RB, Francis CW. Effect of 40-khz ultrasound on acute thrombotic ischemia in a rabbit femoral artery thrombosis model: Enhancement of thrombolysis and improvement in capillary muscle perfusion. Circulation. 2000; 101:2296–2301. [PubMed: 10811598]
8. Wu J, Nyborg WL. Ultrasound, cavitation bubbles and their interaction with cells. Adv Drug Deliv Rev. 2008; 60:1103–1116. [PubMed: 18468716]
9. Altland OD, Dalecki D, Suchkova VN, Francis CW. Low-intensity ultrasound increases endothelial cell nitric oxide synthase activity and nitric oxide synthesis. Journal of thrombosis and haemostasis: JTH. 2004; 2:637–643. [PubMed: 15102020]
10. Sugita Y, Mizuno S, Nakayama N, Iwaki T, Murakami E, Wang Z, Endoh R, Furuhata H. Nitric oxide generation directly responds to ultrasound exposure. Ultrasound Med Biol. 2008; 34:487–493. [PubMed: 17933454]
11. Konno S, S N, Saijo Y, Yambe T, Sato M, Nitta S. Low-intensity ultrasound induces a transient increase in intracellular calcium and enhancement of nitric oxide production in bovine aortic endothelial cells. IFMBE Proceedings. 2009; 23:1989–1992.
12. Krasovitski B, Kimmel E. Shear stress induced by a gas bubble pulsating in an ultrasonic field near a wall. IEEE Trans Ultrason Ferroelectr Freq Control. 2004; 51:973–979. [PubMed: 15344403]

13. Bertuglia S. Increase in capillary perfusion following low-intensity ultrasound and microbubbles during postischemic reperfusion. Crit Care Med. 2005; 33:2061–2067. [PubMed: 16148481]
14. Xie F, Lof J, Matsunaga T, Zutshi R, Porter TR. Diagnostic ultrasound combined with glycoprotein iib/iiia-targeted microbubbles improves microvascular recovery after acute coronary thrombotic occlusions. Circulation. 2009; 119:1378–1385. [PubMed: 19255341]
15. Xie F, Slikkerveer J, Gao S, Lof J, Kamp O, Unger E, Radio S, Matsunaga T, Porter TR. Coronary and microvascular thrombolysis with guided diagnostic ultrasound and microbubbles in acute st segment elevation myocardial infarction. J Am Soc Echocardiogr. 2011; 24:1400–1408. [PubMed: 22037348]
16. Huang A, Sun D, Jacobson A, Carroll MA, Falck JR, Kaley G. Epoxyeicosatrienoic acids are released to mediate shear stress-dependent hyperpolarization of arteriolar smooth muscle. Circ Res. 2005; 96:376–383. [PubMed: 15637296]
17. Harada N, Sakamoto S, Niwa Y, Nakaya Y. Involvement of adenosine in vascular contractile preconditioning. Am J Physiol Heart Circ Physiol. 2001; 280:H2911–2919. [PubMed: 11356652]
18. Ryu JC, Davidson BP, Xie A, Qi Y, Zha D, Belcik JT, Caplan ES, Woda JM, Hedrick CC, Hanna RN, Lehman N, Zhao Y, Ting A, Lindner JR. Molecular imaging of the paracrine proangiogenic effects of progenitor cell therapy in limb ischemia. Circulation. 2013; 127:710–719. [PubMed: 23307829]
19. Xie A, Belcik T, Qi Y, Morgan TK, Champaneri SA, Taylor S, Davidson BP, Zhao Y, Klibanov AL, Kuliszewski MA, Leong-Poi H, Ammi A, Lindner JR. Ultrasound-mediated vascular gene transfection by cavitation of endothelial-targeted cationic microbubbles. JACC Cardiovasc Imaging. 2012; 5:1253–1262. [PubMed: 23236976]
20. Belcik JT, Qi Y, Kaufmann BA, Xie A, Bullens S, Morgan TK, Bagby SP, Kolumam G, Kowalski J, Oyer JA, Bunting S, Lindner JR. Cardiovascular and systemic microvascular effects of anti-vascular endothelial growth factor therapy for cancer. J Am Coll Cardiol. 2012; 60:618–625. [PubMed: 22703929]
21. Wei K, Jayaweera AR, Firoozan S, Linka A, Skyba DM, Kaul S. Quantification of myocardial blood flow with ultrasound-induced destruction of microbubbles administered as a constant venous infusion. Circulation. 1998; 97:473–483. [PubMed: 9490243]
22. Mochizuki S, Himi N, Miyasaka T, Nakamoto H, Takemoto M, Hirano K, Tsujioka K, Ogasawara Y, Kajiya F. Evaluation of basic performance and applicability of a newly developed in vivo nitric oxide sensor. Physiological measurement. 2002; 23:261–268. [PubMed: 12051298]
23. Baker KG, Robertson VJ, Duck FA. A review of therapeutic ultrasound: Biophysical effects. Physical therapy. 2001; 81:1351–1358. [PubMed: 11444998]
24. Wei K, Skyba DM, Firschke C, Jayaweera AR, Lindner JR, Kaul S. Interactions between microbubbles and ultrasound: In vitro and in vivo observations. J Am Coll Cardiol. 1997; 29:1081–1088. [PubMed: 9120163]
25. Kobulnik J, Kuliszewski MA, Stewart DJ, Lindner JR, Leong-Poi H. Comparison of gene delivery techniques for therapeutic angiogenesis ultrasound-mediated destruction of carrier microbubbles versus direct intramuscular injection. J Am Coll Cardiol. 2009; 54:1735–1742. [PubMed: 19850216]
26. Buus NH, Bottcher M, Hermansen F, Sander M, Nielsen TT, Mulvany MJ. Influence of nitric oxide synthase and adrenergic inhibition on adenosine-induced myocardial hyperemia. Circulation. 2001; 104:2305–2310. [PubMed: 11696470]
27. Liao JC, Kuo L. Interaction between adenosine and flow-induced dilation in coronary microvascular network. Am J Physiol. 1997; 272:H1571–1581. [PubMed: 9139938]
28. Bickford RH, Duff RS. Influence of ultrasonic irradiation on temperature and blood flow in human skeletal muscle. Circ Res. 1953; 1:534–538. [PubMed: 13106924]
29. Poucher SM. The role of the a(2a) adenosine receptor subtype in functional hyperaemia in the hindlimb of anaesthetized cats. The Journal of physiology. 1996; 492(Pt 2):495–503. [PubMed: 9019545]

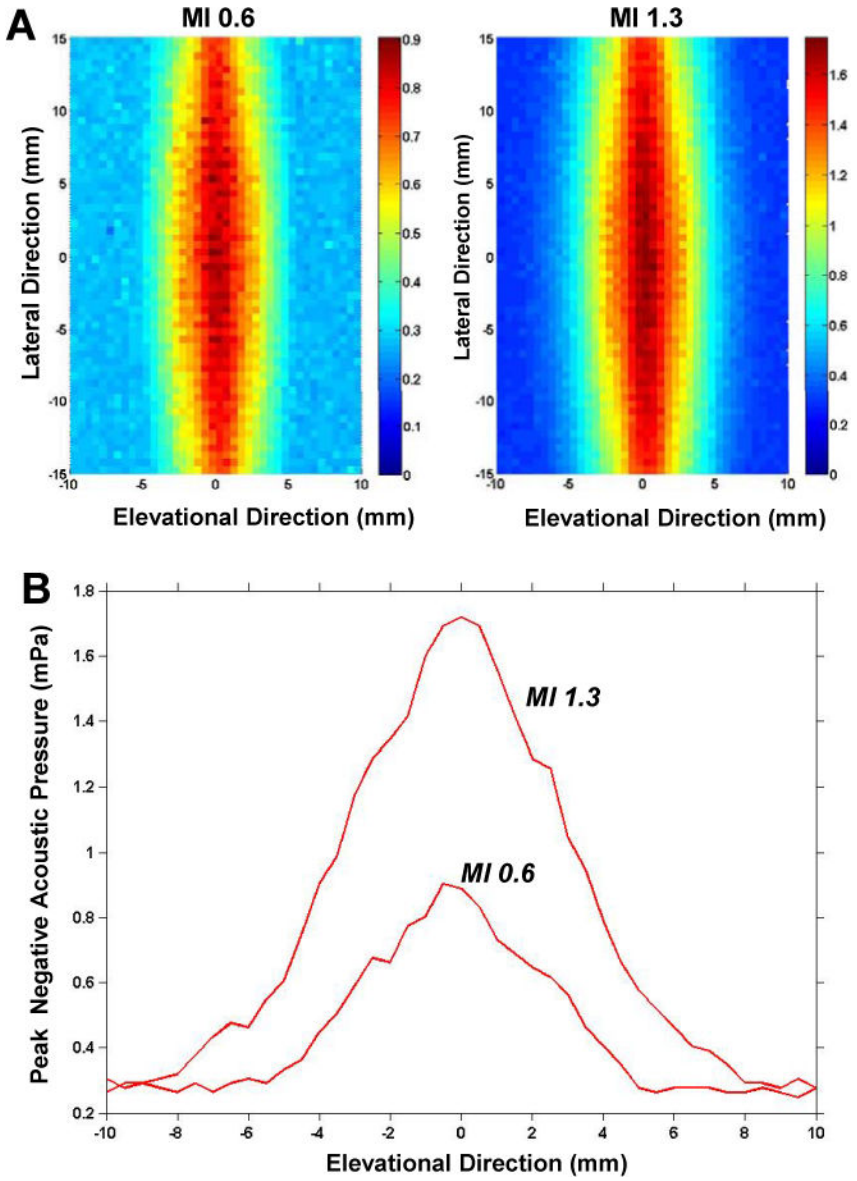

Figure 1.

(**A**) Peak negative acoustic pressure measurements in the lateral and elevational dimension for the two different therapeutic ultrasound conditions. Pressure measurements are color-coded according to the scale denoted in units of MPa. (**B**) Graphic representation of the peak negative acoustic pressure in the elevational dimension at the center of the probe, correlating to the length of muscle exposed when imaging in the short-axis plane.

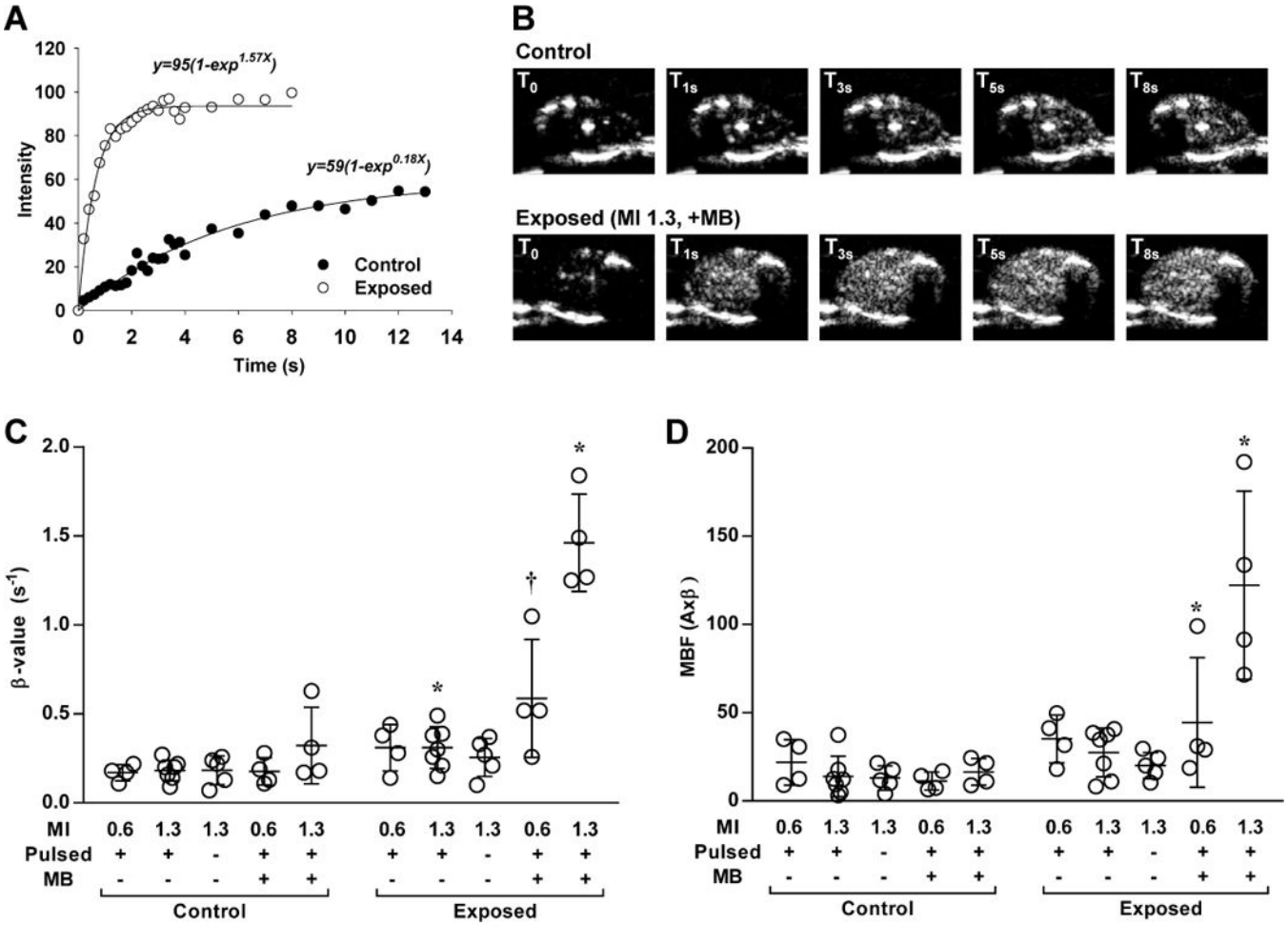

Figure 2.

Contrast ultrasound perfusion data from ultrasound-exposed and control contralateral hindlimbs using 2×10^8 microbubble dosing. (**A**) Examples of time-intensity curves from the adductor muscle group obtained after a destructive pulse sequence in a leg after exposure to ultrasound (MI 1.3) in the presence of MBs and in the contralateral control leg. (**B**) Contrast ultrasound frames obtained from select intervals from the curves in panel A (T_0=immediate post-destruction). (**C and D**) Dot plots with lines representing mean (±SD) of skeletal muscle microvascular blood flux rate (β) and microvascular blood flow (*MBF*) after each of the experimental conditions for the ultrasound exposed and contralateral control limb. MB, microbubble; MI, mechanical index. *p<0.05 versus contralateral control limb; †p=0.05 versus contralateral control limb; all tests were made by non-parametric analysis.

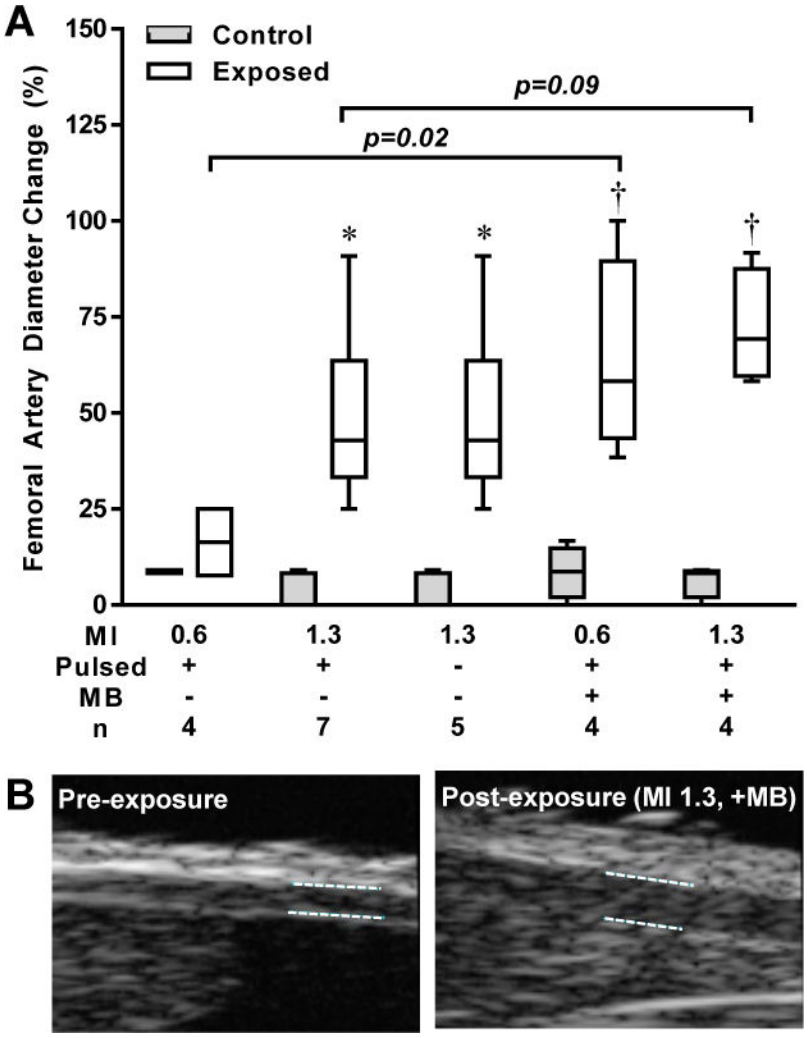

Figure 3.

Femoral artery dilation with ultrasound. (**A**) Box-whisker plots showing median (horizontal line), intequartile range (box), and 5–95th percentile (whiskers) for the percent change in femoral artery diameter measured after each of the experimental conditions for the ultrasound exposed and contralateral control limb. (**B**) Example of a femoral artery at baseline and after exposure to ultrasound (MI 1.3) and MBs. *p<0.05 versus contralateral control limb by paired analysis; †p<0.05 vs. baseline; all tests were made by non-parametric analysis.

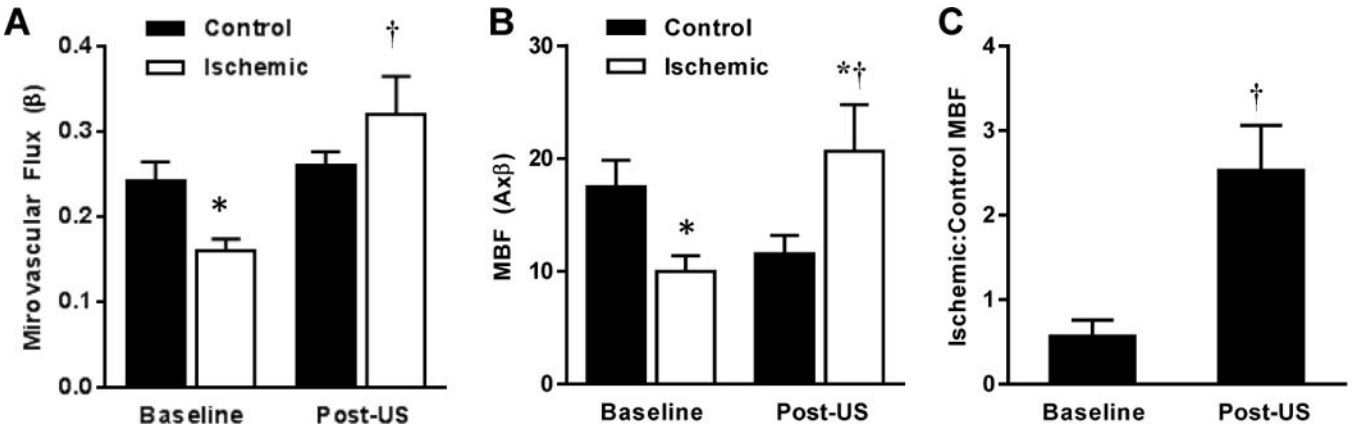

Figure 4.

Mean (±SEM) microvascular flux rate (**A**), microvascular blood flow (MBF) (**B**) and ratio of MBF in the ischemic to contralateral limb (**C**) measured in mice with chronic hindlimb ischemia (n=12). *p<0.05 vs. control limb; †p<0.05 vs. baseline.

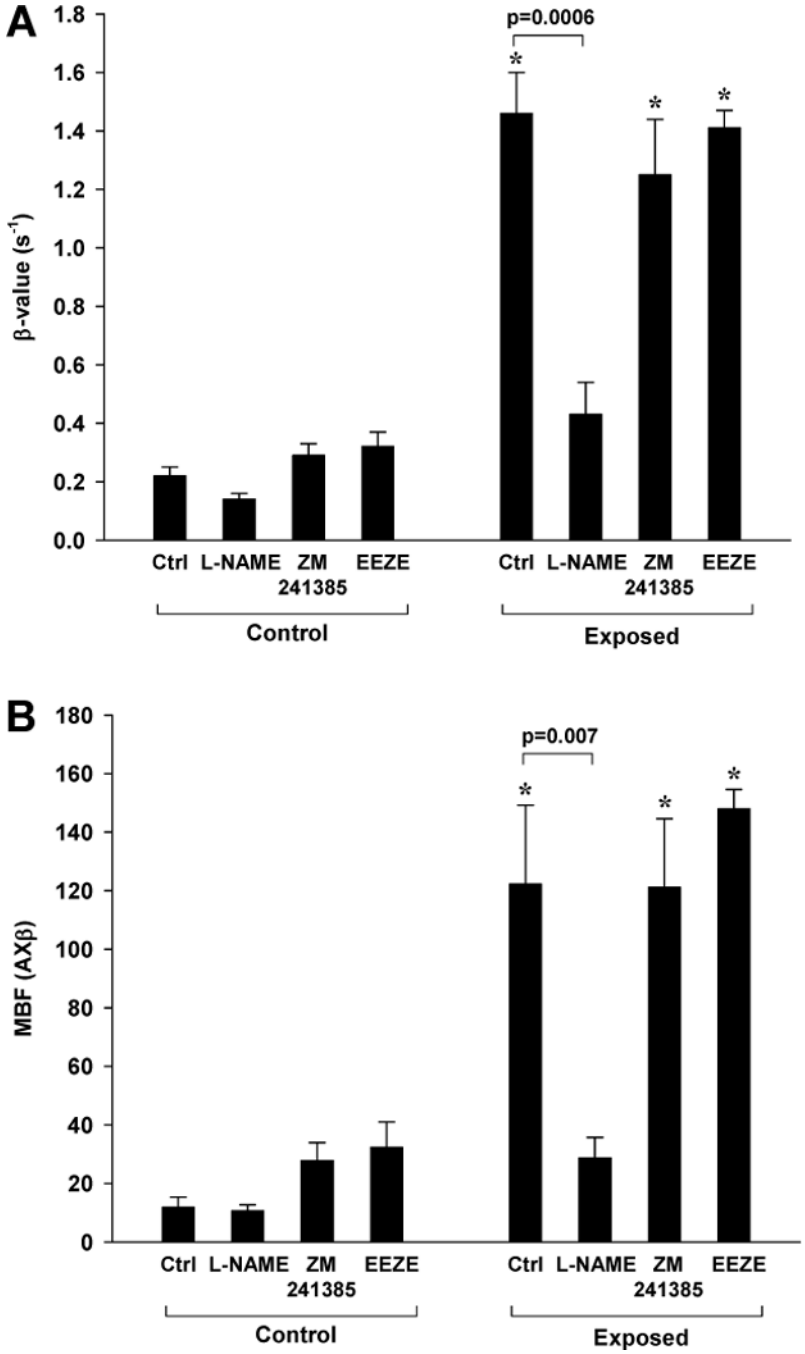

Figure 5.

Contrast ultrasound perfusion data in the presence of inhibitors to vasoactive compounds (n=5 for each condition). Data were obtained after 10 min exposure to intermittent ultrasound (MI 1.3) with MBs alone or after inhibition of NOS (L-NAME), adenosine-A2a receptor signal (ZM241385), or EET signaling (EEZE). Mean (±SEM) data control and ultrasound exposed leg are shown for (**A**) microvascular blood flux rate (β) and (**B**) microvascular blood flow (*MBF*). *p<0.01 versus contralateral control leg.

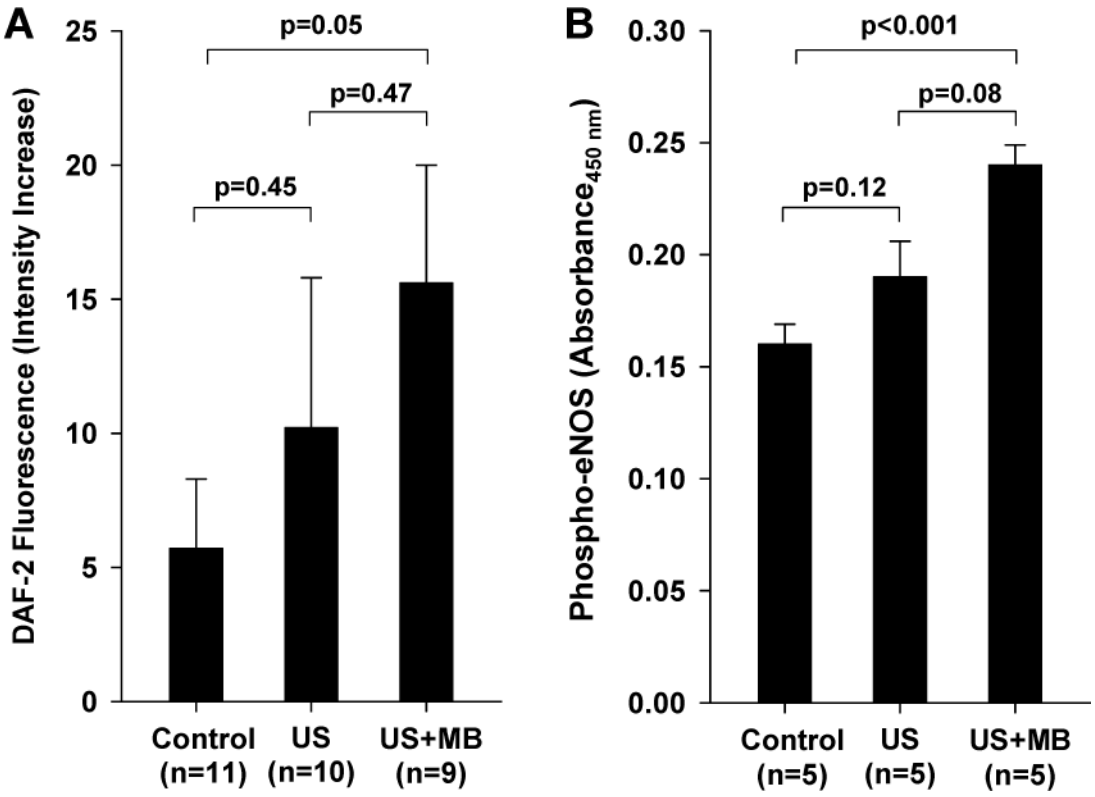

Figure 6.

(**A**) Time dependent increases in fluorescent intensity from the NO indicator DAF-2 from cultured endothelial cells exposed to ultrasound with and without microbubbles (MBs), and from non-exposed time-controlled cells. (**B**) Phosphorylated eNOS by ELISA from control muscle and muscle tissue within the imaging sector in muscle exposed to ultrasound with and without MB injection.

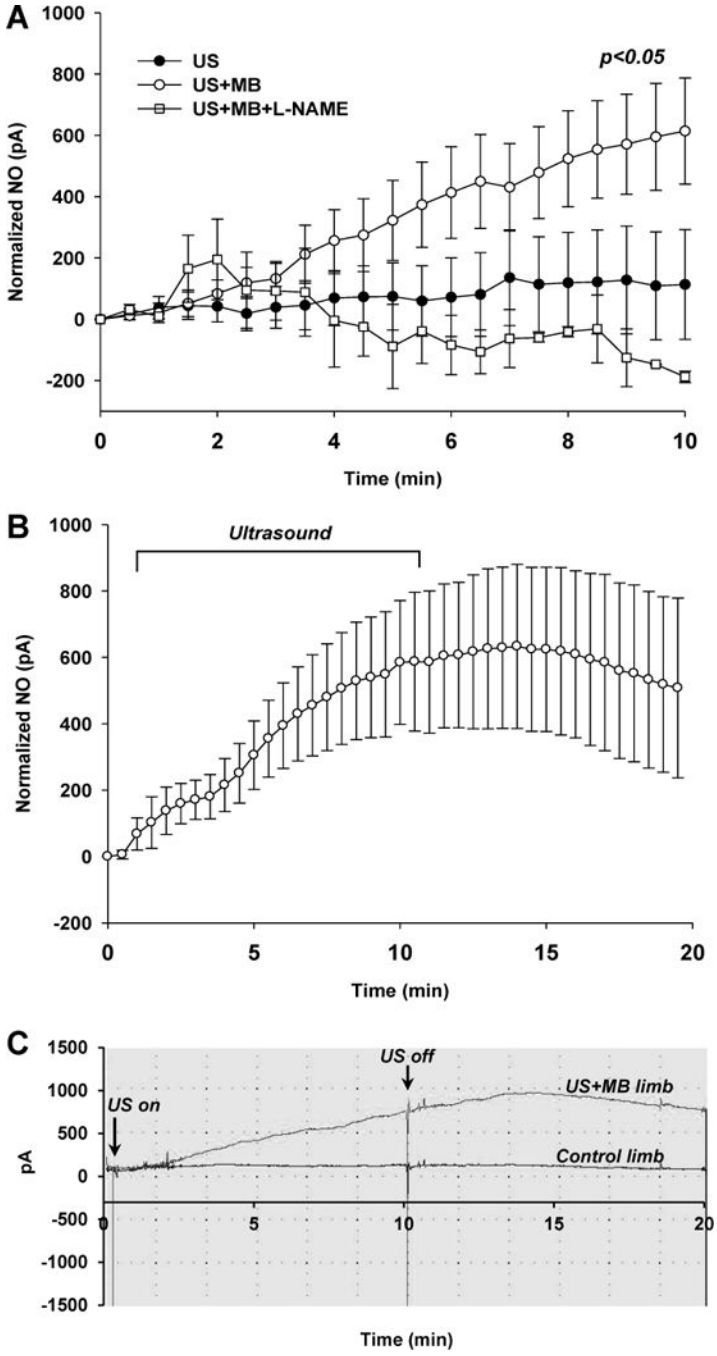

Figure 7.

(**A**) Intramuscular NO production measured by indwelling electrochemical probe after initiating intermittent US alone (n=6), intermittent US with MBs (n=6), and intermittent US with MBs and L-NAME (n=2). Data are normalized to baseline values. (**B**) Intramuscular electrochemical probe detection of NO production after initiating US with MBs where measurements were continued for 10 min after cessation of US (n=4). (**C**) Example of continuous time-dependent NO detection in a limb exposed to ultrasound (MI 1.3) with MBs and the contralateral control limb. Statistical analysis performed with parametric tests.

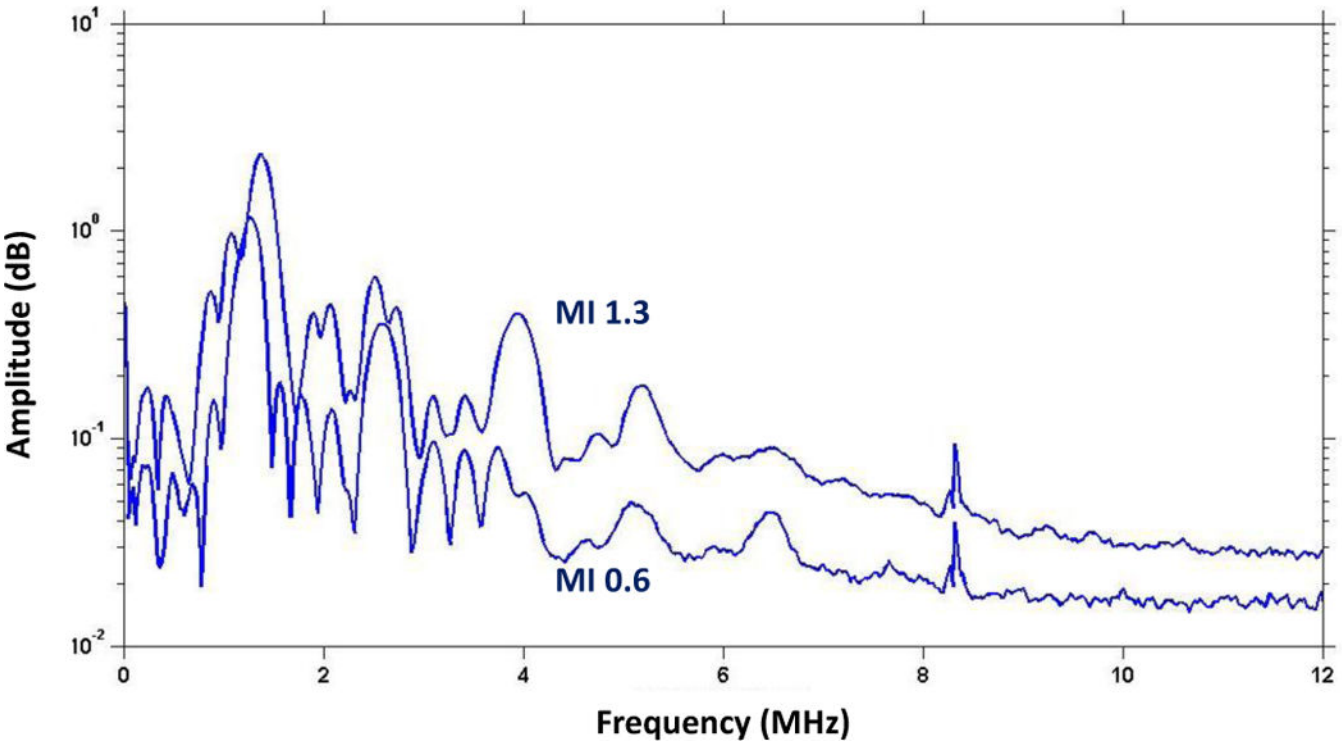

Figure 8.

Frequency-amplitude histograms from passive cavitation detection from microbubbles exposed to ultrasound at MI 0.6 or 1.3. Data are averaged from 250 measurements.